

# Phase Transitions in Lamellar Alkylphosphonate Salts

Wei Gao, Lucy Dickinson, Frederick G. Morin, and Linda Reven\*

Department of Chemistry, McGill University, 801 Sherbrooke St. W.,  
Montreal, QC, Canada H3A 2K6

Received July 15, 1997. Revised Manuscript Received September 19, 1997<sup>®</sup>

The thermal behavior of lamellar metal alkylphosphonate salts is sensitive to the valency of the metal cation. Sodium alkylphosphonates are similar to metal alkanoates, manifesting a small enthalpy transition from a crystalline solid phase to a dynamically disordered solid phase and then a large enthalpy transition to a fluid mesophase. Solid-state <sup>13</sup>C and <sup>31</sup>P NMR spectroscopies show that the large enthalpy transition is associated with melting of the hydrocarbon chains and mobilizing of the phosphonic acid headgroups. The smaller transition, involving the onset of mobility of the all-trans hydrocarbon chains and not the phosphonate headgroups which remain rigid, is detected by DSC and NMR. Above the melting transition, the sample becomes strongly birefringent, indicating the formation of an ordered fluid phase that persists up to the temperature at which the sample begins to lose lattice water. In the case of a divalent metal cation, Zn<sup>II</sup>(O<sub>3</sub>PC<sub>n</sub>H<sub>2n+1</sub>), *n* = 8, 14, 18, the enthalpies of the main transitions are much smaller and the transition temperatures are higher than the sodium alkylphosphonates. Variable-temperature <sup>13</sup>C and <sup>31</sup>P NMR spectra reveal that there is disordering of the hydrocarbon chains at the main transition temperature, but the metal phosphonate network remains intact.

## Introduction

Although there has been considerable interest in the synthesis and the physicochemical properties of metal organophosphonates,<sup>1,2</sup> the thermal behavior of this class of materials is relatively unexplored. These compounds possess layered structures in which the organic groups form bilayers sandwiched between inorganic metal–oxygen–phosphorus polymeric sheets. The exact structure of the metal oxide layer is determined by the choice of metal and reaction conditions. Likewise, the nature of the interlayer region can be controlled by the selection of the organic moiety. The synthetic flexibility of this class of materials has motivated their use in ion exchange, selective sorption, and catalysis.<sup>3</sup> More recently, it has been reported that metal alkylphosphonate salts are potential solid-state phase-change materials (PCMs) which demonstrate latent heat storage equal to the best eutectic salt and organic PCMs but without the odor and hazards of some of these latter materials.<sup>4</sup> In that report, the exact nature of the phase transitions was not investigated but it was assumed that the organic regions undergo solid–solid phase transitions. In particular, the magnesium salts were reported to give rise to the largest latent heats. In addition, a large difference between the thermal behavior of divalent and tetravalent metal alkylphosphonates was noted.<sup>4</sup>

Whereas the thermal behavior of long-chain carboxylates, or soaps, of metal ions has been investigated for many years,<sup>5</sup> there have been no similar studies of the metal phosphonates, other than the report by Almeida and Dixon.<sup>4</sup> In the course of a study of the role of the metal valency on the phase transitions in metal alkylphosphonates, we observe that phase transitions with large latent heats occur in sodium alkylphosphonate salts and that smaller enthalpies are detected for divalent metal alkylphosphonates with the same chain length. In fact, the long-chain phosphonic acids by themselves also display unusual phase behavior that differs from other weakly polar surfactants such as carboxylic acids. Alkylphosphonic acids tend to form lamellar structures due to strong hydrogen bonding among the polar headgroups, and liquid-crystalline phases of *n*-decane and dodecanephosphonic acid/water systems have recently been reported.<sup>6</sup>

Solid-state NMR has been used extensively to characterize the chain packing, dynamics, and phase transitions in layered structure materials such as the perovskite type compounds (C<sub>n</sub>H<sub>2n+1</sub>NH<sub>3</sub>)MCl<sub>4</sub><sup>7</sup>; lamellar polymers,<sup>8</sup> and metal soaps.<sup>9</sup> Only a few metal alkylphosphonate salts have been characterized by solid-

(5) (a) Ubbelohde, A. R.; Michels, H. J.; Duruz, J. J. *Nature* **1970**, *228*, 50. (b) Ubbelohde, A. R. *Nature* **1973**, *244*, 487. (c) Bonekamp, J.; Hegemann, B.; Jonas, J. *Mol. Cryst. Liq. Cryst.* **1982**, *87*, 13. (d) Busico, V.; Ferraro, A.; Vacatello, M. *Mol. Cryst. Liq. Cryst.* **1985**, *128*, 243. (e) Akanni, M. S.; Okoh, E. K.; Burrows, H. D.; Ellis, H. A. *Thermochim. Acta* **1992**, *208*, 1.

(6) (a) Klose, G.; Petrov, A. G.; Volke, F.; Meyer, H. W.; Förster, G.; Rettig, W. *Mol. Cryst. Liq. Cryst.* **1982**, *88*, 109. (b) Schulz, P. C.; Abrameto, M.; Puig, J. E.; Soltero-Martinez, F. A.; Gonzalez-Alvarez, A. *Langmuir* **1996**, *12*, 3082.

(7) (a) Jurga, S.; Macho, V.; Hüser, B.; Spiess, H. W. *Z. Phys. B, Condensed Matter* **1991**, *84*, 43. (b) Kind, R.; Plesko, S.; Arend, H.; Blinc, R.; Zeks, B.; Seliger, J.; Lozar, B.; Slak, J.; Levstik, A.; Filipic, C.; Zagar, V.; Lahajnar, G.; Milia, F.; Chapuis, G. *J. Chem. Phys.* **1979**, *71*, 2118.

(8) Kricheldorf, H. R.; Wutz, C.; Probst, N.; Domschke, A.; Gurau, M. *Multidimensional Spectroscopy of Polymers*; Urban, M. W., Provder, T., Eds.; American Chemical Society: Washington, DC, 1995.

<sup>®</sup> Abstract published in *Advance ACS Abstracts*, November 15, 1997.

(1) (a) Dines, M. B.; DiGiacomo, P. M. *Inorg. Chem.* **1981**, *20*, 92. (b) Martin, K. J.; Squattrito, P. J.; Clearfield, A. *Inorg. Chim. Acta* **1989**, *155*, 7. (c) Cao, G.; Lynch, V. M.; Swinnea, J. S.; Mallouk, T. E. *Inorg. Chem.* **1990**, *29*, 2112. (d) Zhang, Y.; Clearfield, A. *Inorg. Chem.* **1992**, *31*, 2821. (e) Wang, R.-C.; Zhang, Y.; Hu, H.; Frausto, R. R.; Clearfield, A. *Chem. Mater.* **1992**, *4*, 864.

(2) (a) Lynch, V. M.; Mallouk, T. E. *Inorg. Chem.* **1988**, *27*, 2781. (b) Cao, G.; Lee, H.; Lynch, V. M.; Mallouk, T. E. *Solid State Ionics* **1988**, *26*, 63.

(3) (a) Cao, G.; Hong, H.-G.; Mallouk, T. E. *Acc. Chem. Res.* **1992**, *25*, 420. (b) Dines, M. B.; Griffith, P. C. *J. Phys. Chem.* **1982**, *86*, 571.

(4) Almeida, O. J.; Dixon, B. G. *Chem. Mater.* **1995**, *7*, 2039.

state NMR, despite the fact that crystals of the metal phosphonates are difficult to grow for single-crystal X-ray studies. Thompson and co-workers used solid-state NMR techniques to determine the orientation of organic groups in zirconium phosphonates.<sup>10</sup> Harris and Merwin have reported the <sup>31</sup>P and <sup>23</sup>Na solid-state NMR spectra of sodium salts of several diphosphonic acids.<sup>11</sup> Most recently, the relationship of <sup>31</sup>P NMR data with the coordination environment in some zinc phosphonate salts has been examined.<sup>12</sup>

The motivation of this study was to investigate the nature of the large enthalpy phase transitions reported for the metal alkylphosphonates. Solid-state <sup>31</sup>P and <sup>13</sup>C NMR spectroscopies were employed to probe the ionic and hydrocarbon regions of metal salts of alkylphosphonic acids in the various phases detected by differential scanning calorimetry (DSC). We show that the large latent heats are due to complete melting and the subsequent formation of a liquid-crystalline phase in the system where the cations are not strongly bound (Na). In divalent metal phosphonates (Zn, Mn, Mg), the smaller enthalpies are associated with phase transitions occurring exclusively in the hydrocarbon region.

### Experimental Section

**Sample Preparation.** The *n*-alkylphosphonic acids were synthesized by the Michaelis–Arbuzov reaction<sup>13</sup> of the *n*-alkyl bromides and triethyl phosphite. The preparation reported earlier for magnesium alkylphosphonates was followed<sup>4</sup> and is shown by elemental analysis and <sup>31</sup>P NMR to result in the formation of sodium salts. A clear solution of the alkylphosphonic acid was made by dissolving 1.75 g in 800 mL of methanol–H<sub>2</sub>O (75:25 by volume) mixed solvent at 60–70 °C. When the alkylphosphonic acid solution was initially mixed with 80 mL of an aqueous solution containing an equivalent amount of MgCl<sub>2</sub>, a precipitate of poorly crystalline magnesium alkylphosphonate immediately formed. Concentrated HCl was added dropwise to the above solution until the precipitate dissolved and the solution turned clear. The excess HCl was neutralized by adding a 2 M NaOH aqueous solution. The addition of 2 M NaOH was stopped immediately before precipitation occurred. Elemental analysis showed that under these conditions, complete exchange of the Mg cations by Na occurred. We found that a low pH of 2, as used by Almeida and Dixon<sup>4</sup> for the reaction solution, results in the formation of sodium salts rather than magnesium complexes. A pH of 5–6 is necessary for the complete exchange of sodium with magnesium. The reaction was kept at 60–70 °C with stirring for 1 day and then cooled to room temperature during which planar crystallites slowly precipitated. The precipitate was washed with hot methanol–H<sub>2</sub>O mixed solvent and dried under vacuum. In the case of sodium, complete conversion of the long-chain phosphonic acids to the salt requires a gradual and complete evaporation of the solvent.<sup>15</sup> For octadecylphosphonic acid (NaODPA), the elemental analysis of 3.65% Na, 8.79% P, 61.41% C, 11.75% H, and 0.019% Mg agrees with a formula of Na(HO<sub>3</sub>PC<sub>18</sub>H<sub>37</sub>)<sub>2</sub>·H<sub>2</sub>O. Despite the low sodium content indicated by the elemental analysis, the <sup>31</sup>P NMR

spectra showed resonances only for mono- and disodium salts. Although it would be desirable to compare our results with a fully exchanged sodium complex, we did not attempt to prepare this sample since the only syntheses of crystalline long-chain disodium alkylphosphonate salts described in the literature consisted of reacting the alkylphosphonic acid with a saturated salt solution over a period of 6 months.<sup>15</sup>

Zinc, magnesium, and manganese alkylphosphonate salts were prepared by following the procedure used by Mallouk and co-workers.<sup>2</sup> Briefly, a clear solution of phosphonic acid was mixed with metal salt solution on the basis of a 1:1 metal ion to R–PO(OH)<sub>2</sub> ratio. A white precipitate formed instantly. To this solution, concentrated HCl was added until a clear solution was achieved. With vigorous stirring, 0.2 M aqueous NaOH was added dropwise to adjust pH = 5.5. The solution was heated at 100 °C overnight and then kept at 60 °C without stirring for 2 days. This treatment promoted a higher degree of crystallinity. Elemental analysis of these metal phosphonates agree with their formula and showed that no sodium salts were present. For Zn<sup>II</sup>(O<sub>3</sub>PC<sub>8</sub>H<sub>17</sub>) (ZnOPA): expected 37.3% C, 6.65% H; obtained 36.54% C, 6.39% H.

**DSC.** Differential scanning calorimeter thermograms were recorded on a Perkin-Elmer DSC-7 apparatus at a scanning rate of 5 °C/min in a nitrogen atmosphere.

**XRD.** X-ray diffraction patterns were obtained on a Rigaku automated powder diffraction instrument equipped with secondary monochromator with Cu K $\alpha$  radiation at room temperature. An accelerating potential of 40 kV and a filament current of 100 mA were used.

**NMR.** The solid-state 67.92 MHz <sup>13</sup>C and 109 MHz <sup>31</sup>P CP MAS spectra were run on a Chemagnetics CMX-270 NMR spectrometer with a 7 mm double-tuned fast-MAS Doty probe. For <sup>1</sup>H–<sup>13</sup>C cross polarization, the carbon and proton power levels were adjusted to achieve the Hartmann–Hahn match at 60 kHz. The <sup>1</sup>H 90° pulse widths were between 3.5 and 4.5 ms, and contact times of 3 ms were used. The samples were typically spun at 3.5–5.5 kHz, and an average of 100–400 scans taken with delay times of 3 s. For the variable-temperature CP MAS experiments, the sample temperature was controlled to within  $\pm 2$  °C by a Chemagnetics temperature controller.

In the 2D wide-line separation pulse sequence (WISE),<sup>14</sup> a <sup>1</sup>H 90° pulse was followed by a proton evolution period, *t*<sub>1</sub>, consisting of 32 increments of 2 ms. After each *t*<sub>1</sub> period, cross polarization, followed by carbon detection with proton decoupling, gives a carbon spectrum which is modulated as a function of *t*<sub>1</sub> by the free induction decay of the associated protons. A second Fourier transform gives a 2D spectrum with high-resolution <sup>13</sup>C CP MAS spectra along the first dimension, and the wide-line proton spectra associated with each carbon along the second axis.

**Optical Microscopy.** The sample for microscopic observation was prepared by dispersing the suspensions of metal phosphonate salts between a clean microscopic slide and a cover slip then drying under vacuum. The optical micrographs were taken on a Nikon OPTIPHOT polarizing microscope with a Linkam THMS600 hot stage under N<sub>2</sub> atmosphere.

### Results

**XRD.** The X-ray diffraction patterns of NaODPA are shown in Figure 1. The strong, evenly spaced peaks in the low-angle region indicate that a layered structure is formed. Single-crystal studies of di- and monosodium alkylphosphonates with shorter chain lengths (Na<sub>2</sub>(O<sub>3</sub>PC<sub>12</sub>H<sub>25</sub>)·4H<sub>2</sub>O, NaHO<sub>3</sub>PC<sub>12</sub>H<sub>25</sub>, NaHO<sub>3</sub>PC<sub>10</sub>H<sub>21</sub>) have been reported.<sup>15</sup> From the 0*k*0 progression of layer axis lines in the XRD powder patterns of NaODPA, the

(9) Feio, G.; Burrows, H. D.; Gerald, C. F. G. C.; Pinheiro, T. J. *Liquid Cryst.* **1991**, *9*, 417.

(10) (a) Burwell, D. A.; Valentine, K. G.; Thompson, M. E. *J. Magn. Reson.* **1992**, *97*, 498. (b) Burwell, D. A.; Valentine, K. G.; Timmermans, J. H.; Thompson, M. E. *J. Am. Chem. Soc.* **1992**, *114*, 4144.

(11) Harris, R. K.; Merwin, L. H.; Hägele, G. *Z. Naturforsch.* **1989**, *44b*, 1407.

(12) Massiot, D.; Drumel, S.; Janvier, P.; Bujoli-Doeuff, M.; Bujoli, B. *Chem. Mater.* **1997**, *9*, 6.

(13) Bhattacharya, A. K.; Thyagarajan, G. *Chem. Rev. (Washington, D.C.)* **1981**, *81*, 415.

(14) (a) Chin, Y.-H.; Kaplan, S. *Magn. Reson. Chem.* **1994**, *S53*. (b) Clauss, J.; Schmidt-Rohr, K.; Adam, A.; Boeffel, C.; Spiess, H. W. *Macromolecules* **1992**, *25*, 5208.

(15) Schulz, P. C. *Anales Asoc. Quím. Argentina* **1983**, *71*, 271. The complex Na<sub>2</sub>(O<sub>3</sub>PC<sub>12</sub>H<sub>25</sub>)·4H<sub>2</sub>O has a triclinic structure with the following crystallographic parameters: *a* = 9.41 Å, *b* = 5.54 Å and *c* = 30.0 Å,  $\alpha$  = 90.124°,  $\beta$  = 93.571°,  $\gamma$  = 93.73°, *Z* = 4. The hydrocarbon chains are tilted by 51° with respect to the *b* axis, which lies along the ionic planes.

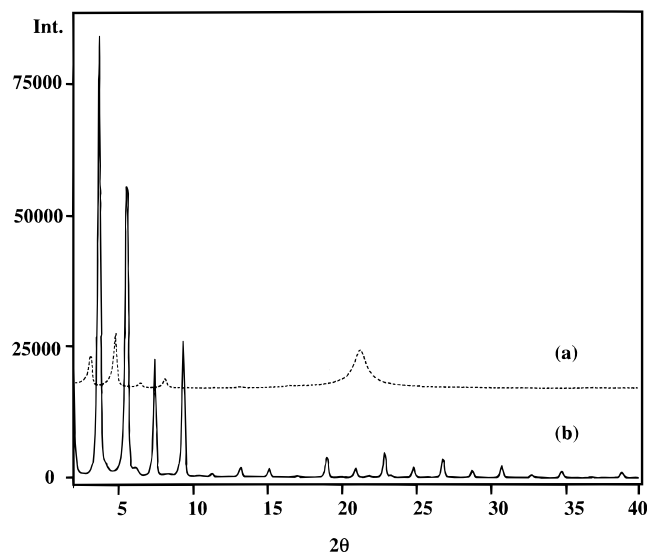


**Figure 1.** X-ray powder diffraction pattern of sodium octadecylphosphonate (a) heated to 160 °C and then cooled to room temperature and (b) virgin sample. The intensity scales are the same in (a) and (b).

interlayer distances are found to be 47.8 and 56.7 Å for virgin and heated samples, respectively. In addition to the increase of the interlayer distance after heating to 160 °C in air, the XRD powder pattern shows a dramatic decrease in the intensities of the reflection peaks in low-angle region with the simultaneous appearance of a new broad peak at  $2\theta \approx 22^\circ$ , indicating a structural rearrangement and the development of defects during the thermal treatment. For ZnOPA, the interlayer spacing is determined to be 24.6 Å and remains unchanged after heating. The doubling of the interlayer distances of NaODPA as compared to ZnOPA may be coincidental; however, the tilt angle of the hydrocarbon chains may be similar for these two lamellar compounds.

**DSC.** The DSC thermograms of NaODPA and ZnOPA are shown in Figure 2. The transition temperatures and enthalpies of the sodium and zinc alkylphosphonates are listed in Table 1. In Figure 2a, a large phase transition with a latent heat of 167 J/g occurs at 131 °C, and two small peaks at 83 and 142 °C with enthalpies of 10 and 0.9 J/g are also detected in the heating scan of NaODPA. Hysteresis is observed for the large phase transition which occurs at 118 °C with  $\Delta H = 105$  J/g in the cooling scan. The large enthalpy phase transitions associated with the melting of solids are observed in all of the sodium phosphonate samples. The transition temperatures are independent of the chain length, but the enthalpies increase linearly with chain length. The small transitions signaling the formation of liquid crystals are detected only in C16, C18, and C20 by DSC. The thermograms and the DSC data shown in Figure 2a and Table 1 demonstrate that the phase transitions observed in sodium alkylphosphonates are not completely reversible.

The transition temperature of ZnOPA is higher and the corresponding enthalpy is smaller compared to the sodium phosphonate of the same chain length. The transitions in ZnOPA are almost completely reversible even after several heating–cooling cycles, but the transitions appear to deteriorate in the longer chain compounds,  $\text{ZnO}_3\text{PC}_{14}\text{H}_{29}$  and  $\text{ZnO}_3\text{PC}_{18}\text{H}_{37}$ .

**$^{13}\text{C}$  Solid-State NMR.** The variable-temperature  $^{13}\text{C}$  NMR spectra of NaODPA are shown in Figure 3 along

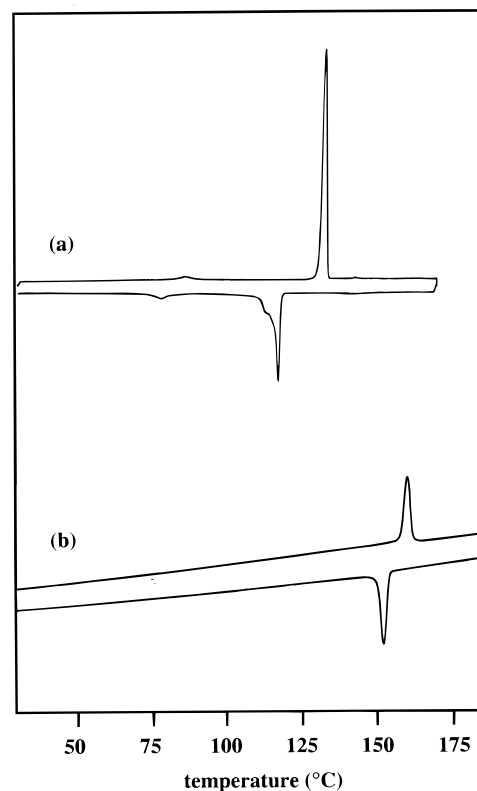


**Figure 2.** DSC thermograms of (a) sodium octadecylphosphonate and (b) zinc octylphosphonate.

**Table 1. Transition Temperatures and Enthalpies for Sodium and Zinc Alkylphosphonate Salts As Observed by DSC in Heating and Cooling Scans**

Na( $\text{HO}_3\text{PC}_n\text{H}_{2n+1}$ )	heating		cooling	
	$T$ (°C)	$\Delta H$ (J/g)	$T$ (°C)	$\Delta H$ (J/g)
$n = 8$	$139 \pm 2^a$	$43 \pm 3$	$60 \pm 2$	$20 \pm 3$
12	$127 \pm 4^c$	$6 \pm 1$		
	$141 \pm 2^a$	$93 \pm 5$	$98 \pm 4$	$65 \pm 3$
14	$59 \pm 4^c$	$2 \pm 0.5$		
	$129 \pm 2^a$	$161 \pm 5$	$114 \pm 3$	$-107 \pm 5$
16	$81 \pm 4^c$	$5 \pm 1$		
	$133 \pm 2^a$	$119 \pm 5$	$114 \pm 2$	$-108 \pm 5$
	$138 \pm 4^b$	$20 \pm 1$		
18	$83 \pm 2^c$	$10 \pm 1$	$81 \pm 2$	$-13 \pm 4$
	$131 \pm 2^a$	$167 \pm 5$	$118 \pm 3$	$-105 \pm 5$
	$142 \pm 4^b$	$0.9 \pm 0.5$	$148 \pm 4$	$-3 \pm 1$
20	$90 \pm 4^c$	$11 \pm 2$	$87 \pm 4$	$-14 \pm 4$
	$132 \pm 2^a$	$178 \pm 5$	$120 \pm 3$	$-112 \pm 5$
	$151 \pm 4^b$	$0.2 \pm 0.1$	$134 \pm 4$	$-7 \pm 2$
22	$101 \pm 4^c$	$27 \pm 2$	$92 \pm 4$	$-11 \pm 3$
	$132 \pm 4^a$	$184 \pm 6$	$123 \pm 4$	$-132 \pm 5$
			$131 \pm 4$	$-7 \pm 2$
<hr/>				
ZnO <sub>3</sub> PC <sub>n</sub> H <sub>2n+1</sub>				
$n = 8$	$158 \pm 2^c$	$23 \pm 2$	$154 \pm 5$	$-29 \pm 4$
14			$64 \pm 4$	$-37 \pm 4$
	$174 \pm 4^c$	$63 \pm 4$	$154 \pm 5$	$-8 \pm 2$
18	$125 \pm 4^c$	$2 \pm 5$	$78 \pm 5$	$-53 \pm 5$
	$173 \pm 4^c$	$55 \pm 3$	$153 \pm 5$	$-14 \pm 2$

<sup>a</sup> Melting. <sup>b</sup> Formation of liquid crystals. <sup>c</sup> Solid–solid transition.

with the peak assignments. The relative populations of trans and gauche conformations influence the  $^{13}\text{C}$  chemical shift of the interior methylene carbons of the alkyl chains. For the  $n$ -alkanes, these carbons resonate at 30 ppm in solution where there are equilibrium populations of trans and gauche conformations, but in the crystalline state they shift downfield to 33–34 ppm for an all-trans conformation.<sup>16</sup> In the room-tempera-

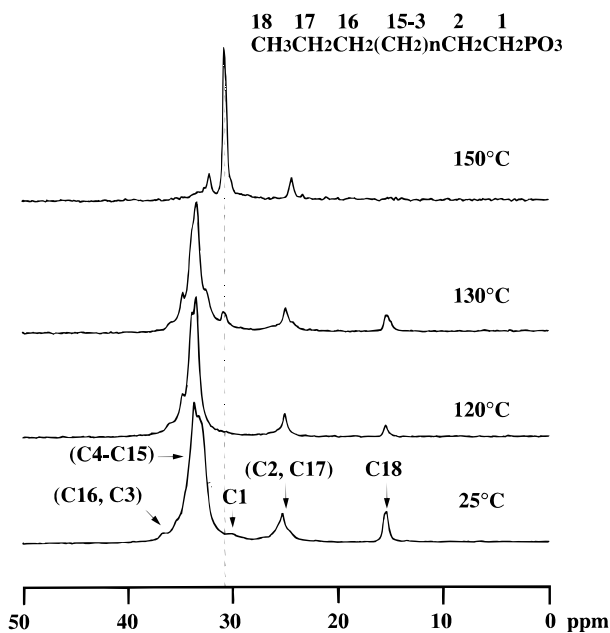


**Figure 3.** Variable-temperature  $^{13}\text{C}$  CP/MAS NMR spectra of sodium octadecylphosphonate. A contact time of 3 ms, a recycle time of 3 s, and average 40 scans were used for each  $^{13}\text{C}$  CP/MAS NMR spectrum.

ture spectrum of NaODPA, the interior methylene carbons are at 33 ppm due to the all-trans conformation of the alkyl chains. The 33 ppm dipolar slice of a 2D WISE spectrum (spectrum not shown) yields a Gaussian proton line shape with fwhh  $\sim 63$  kHz, demonstrating that the alkyl chains are completely rigid at 22 °C. The 1D  $^{13}\text{C}$  CPMAS NMR spectrum at 120 °C, above the first DSC transition, shows that the peaks have narrowed and the resonance for the inner methylenes has split and shifted downfield slightly by  $\sim 0.5$  ppm. At this temperature, the proton line width is reduced to fwhh  $\sim 39$  kHz, signaling the onset of chain rotation. At 130 °C, the  $^{13}\text{C}$  NMR spectrum still shows a strong peak at 33 ppm; however, the small resonance at 30.5 ppm marks the development of gauche defects. At 150 °C, the  $^{13}\text{C}$  resonances are narrow, no longer cross polarize efficiently due to high molecular mobility as indicated by the disappearance of the signal of the methyl end group and have shifted to values corresponding to the solution chemical shifts. The chemical shifts return to the original values after cooling to room temperature, but the peaks are broadened.

The variable-temperature  $^{13}\text{C}$  NMR spectra of ZnOPA are shown in Figure 4. At room temperature, the interior methylenes of the octyl chains, C4 and C5, are shifted to 34 ppm. Upon heating to 150 °C, all of the peaks become narrow and shift slightly upfield, suggesting an increase in mobility of the alkyl chains. At 170 °C, the interior methylene resonance (C4, C5) shifts from 34 to 31.9 ppm, consistent with the presence of a substantial population of gauche conformations above the DSC-detected transition at 158 °C. However, this shift is still 2 ppm downfield of the solution value, which indicates that the alkyl chains are disordered but do not have a totally liquid-like population of trans and gauche conformations. Unlike NaODPA, ZnOPA still

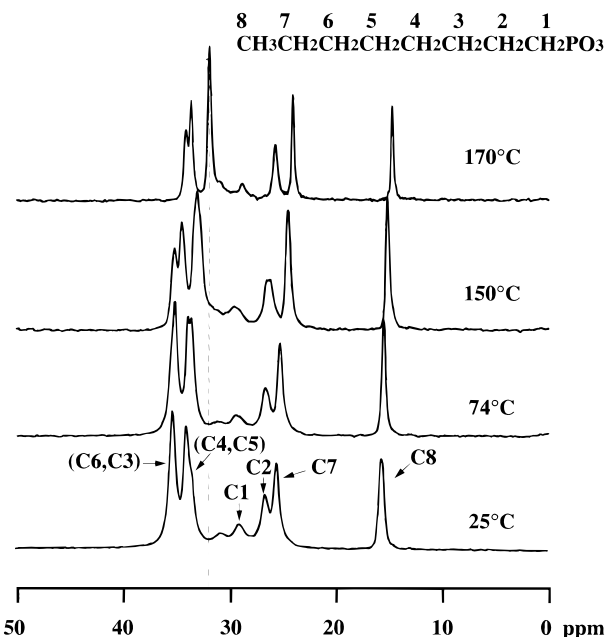


**Figure 4.** Variable-temperature  $^{13}\text{C}$  CP/MAS NMR spectra of zinc octylphosphonate. A contact time of 3 ms, a recycle time of 3 s, and 400 scans were used.

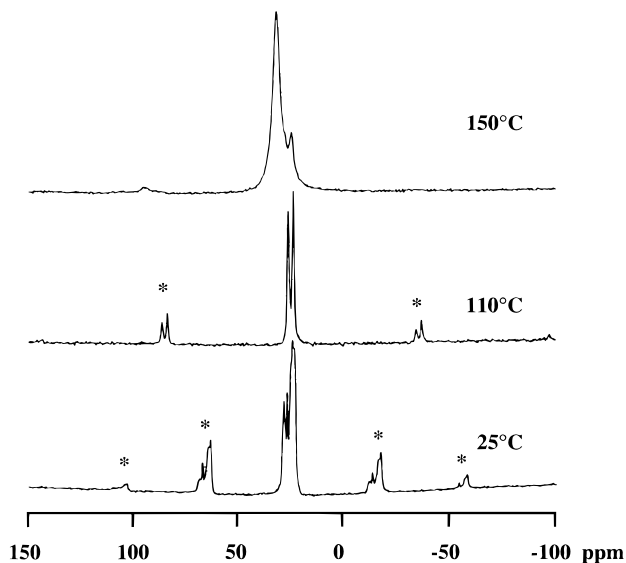


**Figure 5.** Variable-temperature  $^{31}\text{P}$  CP/MAS NMR spectra of sodium octadecylphosphonate. A contact time of 3 ms, a recycle time of 6 s, and 8 scans used. Asterisks indicate spinning sidebands.

shows efficient cross polarization above the transition, demonstrating that the disordered alkyl chains are not highly mobile.

**$^{31}\text{P}$  Solid-State NMR.** The variable-temperature  $^{31}\text{P}$  NMR spectra of NaODPA and ZnOPA are shown in Figures 5 and 6, and the corresponding  $^{31}\text{P}$  chemical shift parameters are given in Table 2. At room temperature, the  $^{31}\text{P}$  CPMAS NMR spectrum of NaODPA (Figure 5) exhibits a large isotropic peak at 23.8 ppm and two smaller resonances at 26.5 and 28 ppm. From 25 to 130 °C both  $^{31}\text{P}$  CPMAS and a single-pulse sequence yield the same spectrum except the smaller peak at 28 ppm gradually disappears. A previous study<sup>17</sup> shows that the  $^{31}\text{P}$  chemical shift of mono- and disodium tetradecylphosphonates are at 28 and 21.9 ppm in solution, but the disappearance of the peak at

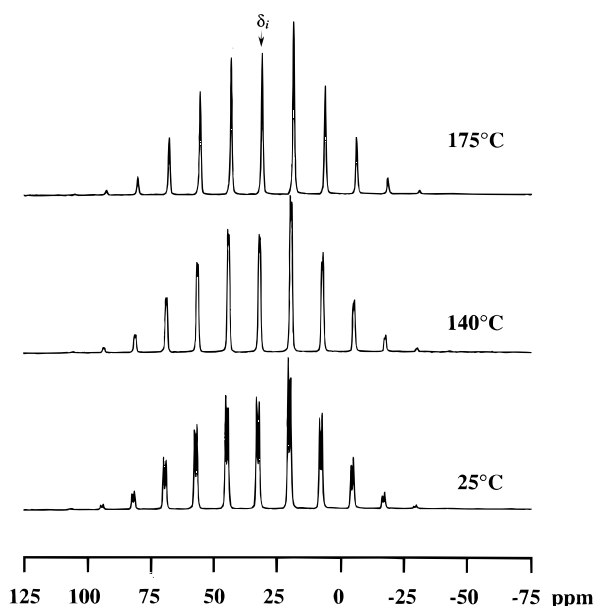


**Figure 6.** Variable-temperature  $^{31}\text{P}$  CP/MAS spectra of zinc octylphosphonate. A contact time of 2 ms, a recycle time of 3 s, 64 scans, and spinning rate of 1.5 kHz were used. The isotropic peak,  $\delta_i$ , is indicated, the other peaks are spinning sidebands.

28.1 ppm in NaODPA with the simultaneous enhancement of signal at 26.5 ppm upon slight heating suggest that the resonance at 28.1 ppm may be due to a weak association between sodium ion and phosphonic acid, whereas the chemical shifts at 26.5 and 23.8 ppm correspond to mono- and disodium coordination environments. Above 130 °C the  $^{31}\text{P}$  CPMAS signals become weak, due to the onset of motion of the phosphonate headgroups. A single-pulse spectrum at 150 °C reveals the appearance of a narrow peak at 31.6 ppm with no spinning sidebands. This chemical shift is very close to that of pure phosphonic acid. Upon cooling, the  $^{31}\text{P}$  CP MAS spectrum returns to the original shift and sideband array, but the peaks are broader.

The variable-temperature  $^{31}\text{P}$  CPMAS NMR spectra of ZnOPA, shown in Figure 6, contrast sharply with that of the sodium complex. Upon heating, the only change detected is a broadening of the peaks. Above main transition temperature, the spinning sideband array is identical with the one at room temperature.

**Optical Microscopy.** The birefringence images of NaODPA at room temperature and at 160 °C are given in Figure 7. At room temperature, the regularly shaped platelike crystallites of NaODPA show a birefringence pattern characteristic of a crystalline solid. No pronounced changes are observed until the main transition at 132 °C, when the platelets melt into droplets and the birefringence disappears. At 148 °C, a strong fanlike birefringence develops and gradually disappears at 180 °C, the temperature at which the lattice water is lost. Upon cooling, the crystalline birefringence pattern is again observed. In contrast, the crystalline birefringence patterns of the divalent metal alkylphosphonates (Zn, Mg, Mn) made at pH = 5.5 do not change upon heating, other than becoming more intense at high temperatures. No fluid phases are observed above the main transition temperatures. Unlike the metal salts,

the pure alkylphosphonic acids become isotropic liquids above their melting temperatures.

## Discussion

**Sample Preparation and DSC Thermograms.** Highly crystalline long-chain metal alkylphosphonates are difficult to prepare. We found that the previously reported preparation of long-chain metal alkylphosphonates using rapid precipitation<sup>4</sup> results in the formation of microcrystalline or amorphous material. Careful control of the pH of the reaction solution to prevent rapid precipitation results in a large increase in both the crystallinity and the latent heat along with the elimination of the multiple peaks in the DSC thermograms reported by other groups in poorly crystalline metal phosphonates.<sup>2b,4</sup> For all metal phosphonates, the interlayer spacing, crystallinity, composition, and particle size are significantly affected by factors such as pH, cosolvent, and the complexing agents in solution.<sup>3</sup> This may account for the variability of the data reported from different groups. For example, the zinc octylphosphonate made at pH = 7.5 shows no transition in the temperature range 25–200 °C, whereas a sample made by rapid mixing without adjusting the pH displays broad multiple transitions over a wide temperature range, despite the fact that these two samples have the same compositions as evidenced by the elemental analysis. We observe little variation in the main transition temperatures of the sodium alkylphosphonate samples: this transition occurs between 130 and 140 °C for sodium alkylphosphonates with chain lengths of  $n = 8$ –22. This trend, also seen in sodium alkanoates, indicates that the electrostatic forces dominate over the weaker van der Waals interactions between chains. Similarly, the pure alkylphosphonic acids (C8–C22) all melt between 95 and 105 °C. However, as expected, a linear increase in the latent heat for the even chain lengths  $n = 8$ –22 in the sodium salts is observed. Although no odd numbered chain lengths were examined in this study, an even–odd effect was reported in the earlier study by Almeida and Dixon.<sup>4</sup>

Compared with the sodium complexes, zinc phosphonates show higher transition temperatures due to stronger ionic bonding but also much smaller enthalpies (Table 1). We studied several other divalent metal octyl- and octadecylphosphonates (Mg, Mn) by DSC and optical microscopy. The magnesium and manganese alkylphosphonates had lower crystallinities and display multiple transitions, similar to the DSC data reported by Mallouk for  $\text{Mg}(\text{O}_3\text{PC}_{12}\text{H}_{25})$ .<sup>2</sup> The latent heats, however, were of the same magnitude as the zinc salts. More importantly, the birefringence patterns upon heating were very similar to the zinc phosphonates, and no fluid phases were detected.

**Room-Temperature NMR.** The  $^{31}\text{P}$  NMR spectra reveal which reaction conditions result in highly crystalline metal phosphonate salts. Multiple transitions in the DSC thermograms, an amorphous peak in the XRD pattern, and a  $^{31}\text{P}$  chemical shift identical with pure phosphonic acid demonstrates that rapid mixing of metal ions and phosphonic acids results in poorly crystalline material with incomplete conversion to the salt. For all the sodium phosphonate samples prepared by slow precipitation through careful adjustment of the pH, sharp transitions,  $\sim 30$  °C higher than the melting

(17) Moedritzer, K.; Irani, R. R. *J. Inorg. Nucl. Chem.* **1961**, *22*, 297.

**Table 2.**  $^{31}\text{P}$  Chemical Shift Parameters of Na and Zn Phosphonates<sup>d</sup>

compound	$\delta_{\text{iso}}^a$ (ppm)	$\eta^a$	$\Delta\sigma^b$	$\delta_{11}$ (ppm)	$\delta_{22}$ (ppm)	$\delta_{33}$ (ppm)	$\eta_e^c$
ODPA	31.3	0.3	-81	63.9	46.3	-25.6	1.7
NaODPA	26.2	0.5	-105	77.8	44.8	-44.0	1.5
	22.2	0.6	-126	88.9	39.7	-61.9	1.4
ZnO <sub>3</sub> PC <sub>8</sub> H <sub>17</sub>	33.6	1.1	-64	79.2	30.5	-9.0	0.9
	32.6	1.1	-66	79.9	29.6	-11.7	0.9
ZnO <sub>3</sub> PC <sub>14</sub> H <sub>29</sub>	33.8	1.1	-65	79.5	31.8	-9.7	0.9
	32.6	1.0	-68	78.5	32.0	-12.7	1.0
ZnO <sub>3</sub> PC <sub>18</sub> H <sub>37</sub>	33.8	1.0	-65	78.2	32.9	-9.7	1.0
	32.7	1.0	-67	77.4	32.4	-11.8	1.0

<sup>a</sup> Chemical shift asymmetry ( $\eta$ ) =  $|\delta_{22} - \delta_{11}|/|\delta_{33} - \delta_{\text{iso}}|$ . <sup>b</sup> Chemical shift anisotropy ( $\Delta\sigma$ ) =  $\delta_{33} - 1/2(\delta_{11} + \delta_{22})$ . <sup>c</sup> Extended chemical shift asymmetry ( $\eta_e$ ) =  $\eta$  ( $\Delta > 0$ ); ( $\eta_e$ ) =  $2 - \eta$  ( $\Delta < 0$ );  $\Delta = \delta_{33} - \delta_{\text{iso}}$ .<sup>12</sup> <sup>d</sup> The shifts are referenced to 85% phosphonic acid using (2*R*,3*R*)-+bis(diphenylphosphino)butane as a secondary standard whose upfield peak is assigned a shift of -13.0 ppm.

temperature of the pure phosphonic acids, are detected along with  $^{31}\text{P}$  isotropic shifts corresponding to mono- and disodium salts. A complete deprotonation of the long-chain alkylphosphonic acids is difficult to obtain, and the pure disodium salts are formed only after slow evaporation of all the solvent.<sup>15</sup> Since our samples were precipitated from a water-methanol mixed solvent, both mono- and disodium groups are present.

The  $^{31}\text{P}$  isotropic chemical shifts of the zinc alkylphosphonates are slightly downfield of the pure phosphonic acids, similar to the previously reported spectrum of zinc ethylphosphonate.<sup>12</sup> A single-crystal study of zinc phenylphosphonate<sup>1b</sup> showed that zinc is in an octahedral coordination with one water molecule filling out the metal coordination shell. Other studies demonstrated that the coordinated water is lost at 70 °C in zinc methylphosphonate and at 80 °C in zinc phenylphosphonate.<sup>18</sup> The dehydrated zinc phosphonates no longer absorb water due to their relatively stable five-coordination. Our TGA curves of the long-chain zinc alkylphosphonates (C8, C14, C18) showed no water loss and the OH bending mode at 1600  $\text{cm}^{-1}$  in IR spectra is not present, indicating the absence of a water molecule in the coordination shell in these samples.<sup>19</sup>

The changes of the local symmetry of the phosphonate headgroup are reflected by the  $^{31}\text{P}$  CSA parameters, listed in Table 2. *N*-Alkylphosphonic acids have a nearly axially symmetric phosphorus shielding tensor ( $\eta \sim 0$ ) due to rapid proton transfer between the P-O groups. Other phosphonic acids in which this proton transfer does not occur have larger asymmetry parameters,  $\eta \sim 0.5$ – $0.8$ , since strong hydrogen bonding deforms the tetrahedral structure of the  $\text{PO}_3\text{H}_2$  group.<sup>20</sup> Upon complexation of octadecylphosphonic acid with Na, the CSA parameter  $\Delta\sigma$  increases from 81 to 105–126 ppm and the asymmetry factor  $\eta$  increases from 0.3 to 0.5–0.6 (Table 2). In a solid-state NMR study of several sodium salts of diphosphonic acids, the tetrasodium salt was found to have an axially symmetric shielding tensor, but the  $^{31}\text{P}$  shielding tensor of the disodium salt is asymmetric since at least one of the oxygens on each phosphorus group is still involved in hydrogen bonding.<sup>11</sup> Likewise, the presence of uncoordinated oxygens in NaODPA, accounts for the increase in the asymmetry factor.

Compared to the pure phosphonic acids and their sodium salts, zinc alkylphosphonates have a relatively

large asymmetry parameter  $\eta = 1.0$ – $1.1$ . The axially asymmetric  $^{31}\text{P}$  shielding tensor indicates that the three oxygen atoms of phosphonate headgroups are not equivalent. The relationship between the coordination state and solid-state  $^{31}\text{P}$  NMR parameters has recently been determined from a NMR study of a number of zinc phosphonates for which single-crystal X-ray data were available.<sup>12</sup> For the connectivity (111) in which each of the three oxygen atoms of the phosphonate unit coordinate to only one zinc atom, the extended asymmetry parameter is  $\eta_e = 0.4$ ; for the connectivity (112) in which one of the oxygen atoms bridges two zinc atoms, the  $\eta_e = 0.8$ ; while for the connectivity (122), two bridging oxygens are present and  $\eta_e = 1.1$ . In our zinc phosphonate samples (C8, C14, C18),  $\eta_e \sim 0.9$ – $1.0$  and the CSA patterns are consistent with a (112) connectivity. Although the assignment of the connectivity in zinc phosphonates (C8, C14, C18) is not unambiguous, at least one oxygen of the phosphonate headgroup bridges to two zinc atoms in these samples.

**Variable-Temperature NMR and Optical Microscopy.** Whereas the first transition observed in the DSC thermogram at 82 °C in NaODPA is a true solid–solid phase transition and no loss of birefringence is observed by optical microscopy, the peak at 132 °C corresponds to a melting transition. The variable-temperature  $^{13}\text{C}$  NMR spectra and the reduced proton line widths show that the transition at 83 °C involves the onset of motion of the all-trans chains. These two transitions are also clearly observed in a variable-temperature Raman and infrared study which will be discussed in a future report.<sup>19</sup> The possible motions associated with the first small transition at 83 °C include rotation about the chain axis and/or untilting with respect to the inorganic layers since the chains retain the all-trans conformation in this phase. Such motions have been detected in the lamellar alkylammonium perovskites  $(\text{C}_n\text{H}_{2n+1}\text{NH}_3)\text{-MCl}_4$  in which melting of the hydrocarbon chains is also observed.<sup>7</sup> The tilt angle of the chain axis estimated for magnesium long-chain metal phosphonates  $\text{Mg}(\text{O}_3\text{-PC}_n\text{H}_{n+1})\cdot\text{H}_2\text{O}$ ,  $n = 4$ – $12$  is quite large,  $52^\circ$ ,<sup>2</sup> and untilting of the chains would provide considerable free volume for chain reorientations. Such a transition would involve an increase in the interlayer distance and variable-temperature XRD measurements are currently underway to see if such a structural change occurs. Since the spinning sideband pattern of the  $^{31}\text{P}$  NMR spectrum of NaODPA does not change, the phase transition at 83 °C involves only reorientations of the hydrocarbon chains. This dynamic behavior differs from pretransitions in other systems such as the *n*-alkylam-

(18) (a) Cao, G.; Mallouk, T. E. *Inorg. Chem.* **1991**, *30*, 1434. (b) Frink, K. J.; Wang, R.-C.; Colon, J. L.; Clearfield, A. *Inorg. Chem.* **1991**, *30*, 1438.

(19) Gao, W.; Dickinson, L.; Reven, L., unpublished results.

(20) Klöse, G.; Möps, A.; Grossmann, G.; Trahms, L. *Chem. Phys. Lett.* **1990**, *175*, 472.

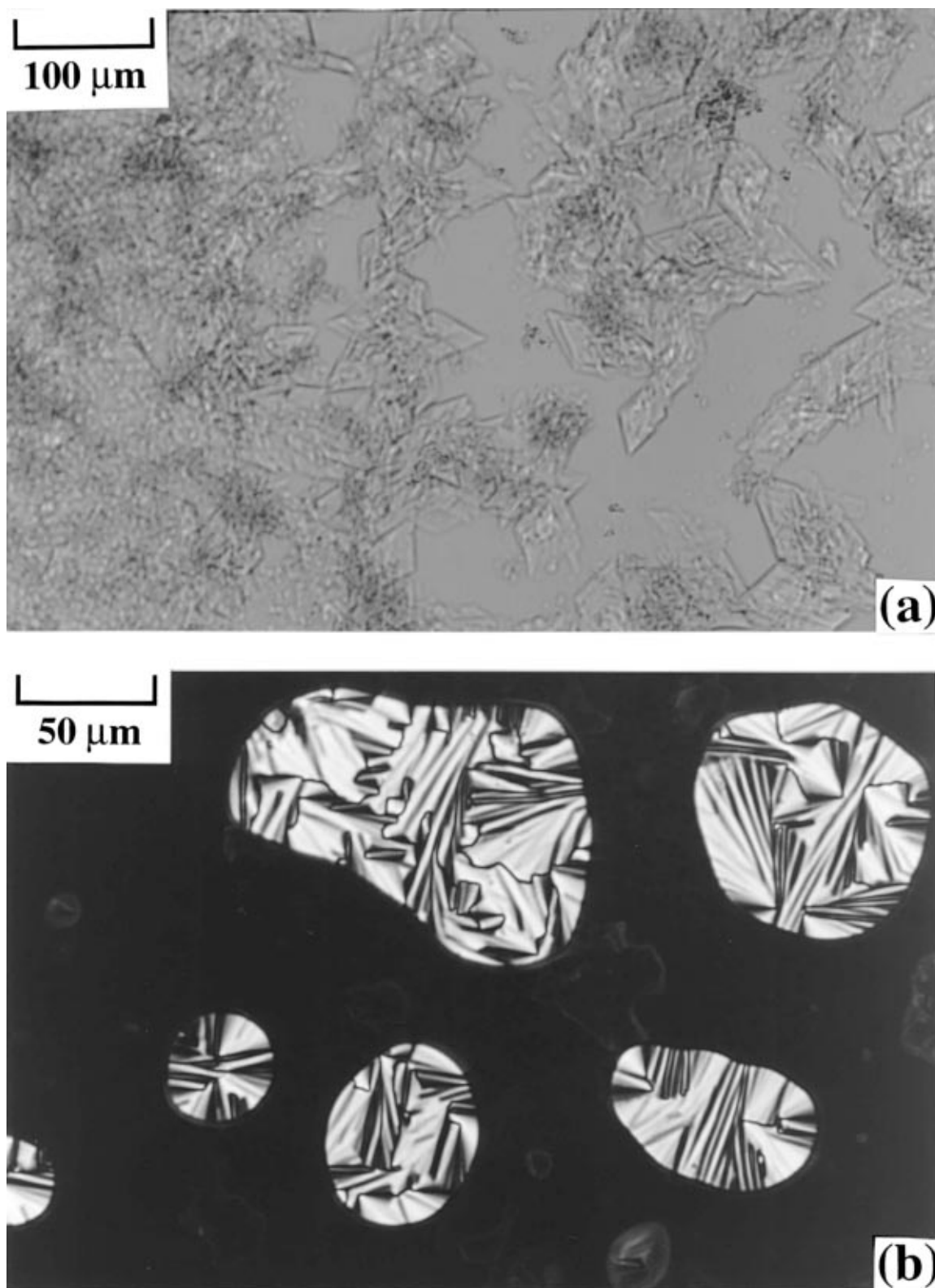


**Figure 7.** Birefringence images of sodium octadecylphosphonate at (a) room temperature and (b) at 160 °C.

monium halides which involve reorientation of both the hydrocarbon chain and the  $\text{NH}_3$  headgroup.

At the main transition at 132 °C, the  $^{31}\text{P}$  MAS NMR spectrum also becomes liquid-like, i.e., the sidebands vanish and a single narrow resonance appears at 31.8 ppm, close to the value of the phosphonic acid alone. This downfield shift of the  $^{31}\text{P}$  resonance indicates that the phosphonate headgroups become very mobile in the high-temperature phase. The sodium alkylphospho-

nates appear to form a fluid mesophase like those observed for metal carboxylates. The fanlike birefringence pattern observed above 148 °C is similar to that observed for smectic liquid crystals. A bilayer structure is probably retained in this ordered fluid phase, as is the case for many of the metal carboxylate mesophases.<sup>5</sup>

In contrast to the sodium phosphonates, the transitions in the zinc alkylphosphonates are true solid–solid transitions. Although chain disordering is observed by

variable-temperature  $^{13}\text{C}$  NMR, no fluid phase is detected by optical microscopy above the main transition temperature. The unchanged  $^{31}\text{P}$  CSA sideband array and powder pattern above the main transition temperature demonstrate that the linkages between the zinc ions and phosphonate headgroups remain rigid. The retention of the metal phosphonate inorganic layer accounts for the relatively low latent heats in zinc phosphonate salts as compared to those of sodium phosphonates of the same chain length, which completely reorganize to form a fluid mesophase.

We were unable to reproduce the DSC data reported by Almeida and Dixon<sup>4</sup> for the Mg alkylphosphonates since we found that a low pH of 2 of the reaction solution results in the formation of sodium salts rather than magnesium complexes. A pH of 5–6 is necessary for the complete exchange of sodium with magnesium. The DSC data as a function of chain length of the sodium alkylphosphonates match those reported previously for the magnesium salts, suggesting that sodium, rather than magnesium salts were formed at pH 2 used in that earlier study. For the zinc complexes, our measured latent heats did not differ greatly from the previous reported values. Compared to magnesium, zinc and manganese were found to complex more readily with phosphonic acids. Therefore, we attributed the anomalously large latent heats reported in the other study for magnesium alkylphosphonates to the presence of sodium salts.

### Conclusions

The earlier study noted a large difference in the thermal behavior of divalent and tetravalent metal alkylphosphonates.<sup>4</sup> In the case of the vanadium alkylphosphonates, the transitions are broad, the latent

heats are quite small and do not increase with chain length, and there is no hysteresis in the DSC thermograms. This difference is obviously due to the extremely strong ionic bonds present in the higher valency metal phosphonates. In the divalent zinc phosphonates, the phosphonate metal linkages remain intact, and the smaller enthalpy transitions observed are solely due to solid-state disordering of the alkyl chains. Since a high degree of crystallinity is much more difficult to achieve in the case of the higher valency metal phosphonates, this may also account for the low transition enthalpies observed in these samples.

In regards to utilization of metal alkylphosphonates as solid-state phase-change materials, the large latent heats were observed only for the sodium salts and are due to the formation of a fluid mesophase rather than a true solid–solid transition. Carefully prepared divalent metal alkylphosphonates do undergo true solid-state transitions, but the corresponding enthalpies are rather small in comparison with some of the layered perovskite type materials. However, the thermal stability of the divalent metal phosphonate network, along with the reversibility of the organic layer phase transition, is relevant to the growing number of applications of metal organophosphonates in other areas, particularly in the field of catalysis.

**Acknowledgment.** This research was supported by the Natural Sciences and Engineering Council of Canada (NSERC) and the FCAR Nouveaux Chercheurs program, of Quebec. Support from the Commonwealth Foundation for L.D. is gratefully acknowledged. We also thank G. R. Brown for the use of his equipment for the optical microscopy.

CM970502K